# FWI spectral sensitivity analysis in the presence of a free surface

*V. V. Kazei*, B. M. Kashtan, V. N. Troyan, Saint-Petersburg State University, Russia and W. A. Mulder, Shell GSI BV & Delft University of Technology, Netherlands*



## SUMMARY

Low frequencies play a crucial role in the convergence of full waveform inversion to the correct model in most of its current implementations (Baeten et al., 2013). Unfortunately, low frequencies are often not present in the data. Mora (1989), however, showed that a reflector below the target area may help in recovering some of its long-wavelength information. We earlier analyzed the contributions of various wave types to the wavenumber spectrum of a velocity perturbation in a simple model of two halfspaces (Kazei et al., 2013b). Here, we extend this spectral sensitivity analysis to the case with a free surface, which generates multiples and ghosts. The multiples increase the total energy in the wavefield and can potentially improve the sensitivity and resolution of full-waveform inversion. Our study shows that the inclusion of multiples increases the sensitivity in some parts of the model's spatial spectrum. At the same time, they make the inverse problem more difficult to solve, because the wavenumber spectrum of the wavefield at a given frequency has sensitivity peaks at a discrete wavenumber subset, making it difficult to invert for the other wavenumbers. Its adverse effect can be reduced by simultaneous inversion of a dense set of frequencies in a frequency-domain code or by using a time-domain approach.

## INTRODUCTION

Full-waveform is known to suffer from factors that introduce additional non-linearities into the scattered wavefield. Among those are free-surface related effects. Here, we consider the role of multiples and ghosts in a 2-D marine-type acquisition for the constant-density acoustic case, and try to figure out which spatial wavenumbers in the velocity model can be reconstructed by FWI and how the inversion should be set up to deal with them. The simplest model for marine acquisition – a homogeneous layer over a homogeneous halfspace with a higher velocity – allows for an analytical derivation of Green functions that are easy to analyze. It turns out that the spectral coverage for full-waveform inversion (Mora, 1989) and wavefield spectral sensitivity patterns (Kazei et al., 2013b) can be derived analytically too. Multiples are usually classified as an additional factor of non-linearity for FWI. Our sensitivity analysis, however, shows that they also complicate the linear problem which FWI faces at each iteration. Ghosts are often considered as a modification of the wavelet. Their presence actually slightly simplifies our analysis instead of making it more complicated. Spectral coverage diagrams, originally suggested by Devaney (1984) for diffraction tomography, can also be used to analyze FWI in horizontally uniform starting models (Mora, 1989; Sirgue and Pratt, 2004; Kazei et al., 2013a). The method is based on a simple relation between the observed wavefield spectrum and the velocity perturbation spectrum and requires Green functions in the $f$-$k$ domain to be derived the former. To gain more insight in the effect of multiples on the spectral resolution, we consider background models consisting of one or two acoustic layers over a halfspace.

## FORWARD PROBLEM

A solution of the 2-D constant-density acoustic wave equation in a horizontally layered medium can be represented as (Brekhovskikh and Godin, 1998):

$$\hat{p}(\mathbf{r},t) = \int_{-\infty}^{\infty} dk_x\, e^{-ik_x x} \int_{-\infty}^{\infty} d\omega\, e^{i\omega t}\, p(k_x,z,\omega). \qquad (1)$$

The pressure $\hat{p}(\mathbf{r},t)$ depends on position $\mathbf{r}$ and time $t$ and the transformed pressure $p(k_x,z,\omega)$ on horizontal wavenumber $k_x$, depth $z$ and angular frequency $\omega$. Within a layer with velocity $c_0$, the solution of the wave equation is a linear combination of upgoing $(+)$ and downgoing $(-)$ wavefields of the form $\exp\left(\pm iz\sqrt{k_0^2-k_x^2}\right)$, with $k_0=\omega/c_0$. Note that the chosen Fourier convention is the conjugate of the customary one. In the case of two halfspaces, where the upper one with sources and receivers and scatterers has a velocity $c_0$ and the deeper a velocity $c_1$, the wavefield for a point source at zero depth in the upper halfspace consists of an incident downgoing and a reflected upgoing wavefield:

$$p_0(k_x,z,\omega) = \frac{e^{-iz\sqrt{k_0^2-k_x^2}} + V(k_x)e^{+i(z-2H)\sqrt{k_0^2-k_x^2}}}{-2i\sqrt{k_0^2-k_x^2}}. \qquad (2)$$

The wavefield in the deeper halfspace is downgoing (Brekhovskikh and Godin, 1998):

$$p_1 = [1+V(k_x)]\frac{e^{-iH\sqrt{k_0^2-k_x^2}}}{-2i\sqrt{k_0^2-k_x^2}} e^{-i(z-H)\sqrt{k_1^2-k_x^2}}, \qquad (3)$$

$$V(k_x) = \frac{1-b}{1+b}, \quad b = \sqrt{\frac{k_1^2-k_x^2}{k_0^2-k_x^2}}.$$

Here, $V(k_x)$ is the reflection coefficient, $H$ is the distance between source and the lower halfspace and $k_1=\omega/c_1$ contains the velocity $c_1$ of the deeper halfspace. Note that $|k_x|=|k_1|$ corresponds to the critical angle of incidence. The factor $|1+V(k_x)|$ can increase to 2 for values of $|k_x|$ close to but less than $|k_1|$, boosting the amplitudes of refracted plane waves that travel almost horizontally in the deeper halfspace.

Next, we include a free surface as sketched in Figures 1(a) and (b). If all multiples are included, then the pressure $p$ changes to

$$p' = p\left(1+\sum_{n=1}^{N}\left[-V(k_x)e^{-2iH\sqrt{k_0^2-k_x^2}}\right]^n\right), \qquad (4)$$


DOI http://dx.doi.org/10.1190/segam2015-5898847.1

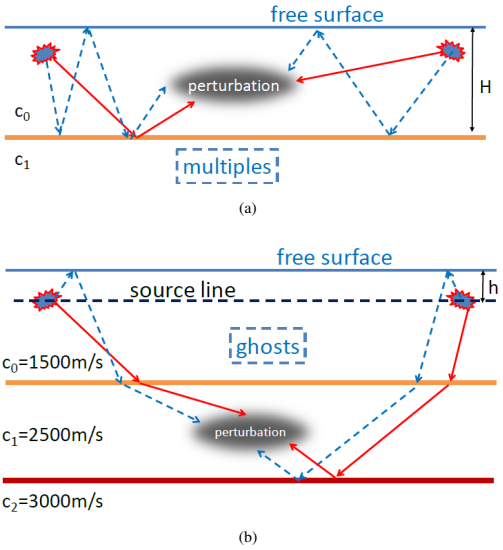


Figure 1: (a) Multiples illuminate a perturbation from all directions and its illumination is improved; (b) ghosts interfere with the useful signal (solid), harming it a bit.

$$p' \xrightarrow{N\to\infty} \frac{p}{1+V(k_x)e^{-2iH\sqrt{k_0^2-k_x^2}}}. \tag{5}$$

The zeros of the denominator on the right-hand side correspond to normal modes. The fundamental mode, which is always present, corresponds to $k_x = k_0$. The existence and the number of higher-order modes depend on the layer thickness – the thicker the layer, the more zeros we have. To avoid convergence problems in equation 4, we limit our investigation to the first-order multiples ($N = 1$). Ghosts, as sketched in Figure 1(b), can be expressed with the same formula as the first-order multiples after replacing $H$ with $h$ and taking $V(k_x) = 1$. If sources and receivers are very close to the free surface, we can simplify the expressions for the pressure by the following approximation, up to $O(h^2)$:

$$p'' = p'e^{ih\sqrt{k_0^2-k_x^2}}\left(1-e^{-i2h\sqrt{k_0^2-k_x^2}}\right) \simeq 2ihp'\sqrt{k_0^2-k_x^2}. \tag{6}$$

Equation 6 shows that, for $h$ much smaller than wavelength, the ghost simply causes cancellation of the square roots in the denominators of equations 2 and 3, which simplifies our final expressions. Thus, the wavenumber spectra of the pressures would be more uniform if we had only ghosts as a result of a free surface inclusion. For larger values of $h$, the ghost compensation technique (Zhang et al., 2012, e.g.) can be applied.

## INVERSION: THEORY

With expression 4 for the wavefield, we can generalize Mora's (1989) technique of sensitivities. The scattered field is determined by the Born approximation. After a Fourier transform in the horizontal source and receiver coordinates, the wavefield perturbation becomes

$$\delta u_{sr}(\omega,k_s,k_r) = \int k_0^2\,\delta W(\mathbf{r})s(\omega)G(\omega,k_s,\mathbf{r})G(\omega,k_r,\mathbf{r})\,d\mathbf{r}, \tag{7}$$

with $\delta W(\mathbf{r})$ a small perturbation of the background squared slowness and with source signature $s(\omega)$. We earlier studied the case of two halfspaces without a free surface (Kazei et al., 2013b). Updating the Green functions according to equations 4 and 6, we obtain a similar but slightly more complicated linear relation between the spatial perturbation spectrum and the transformed data in terms of sensitivities:

$$S(\omega,K_x,K_z) = \left|\frac{\delta u_{sr}\left(\omega,k_s(K_x,K_z),k_r(K_x,K_z)\right)}{s(\omega)\omega^2\delta\widetilde{W}(K_x,K_z)}\right|. \tag{8}$$

Equation 8 describes the relation between the spectra in the wavenumber domain $K_x, K_z$ of the perturbation, $\delta\widetilde{W}(K_x,K_z)$, and the resulting wavefield, $\delta u_{sr}\left(\omega,k_s(K_x,K_z),k_r(K_x,K_z)\right)$. It has this simple form when a horizontally layered background model is assumed. Smooth horizontally uniform models can also be considered by restricting the depth of the perturbation (Kazei et al., 2013a). When the sensitivity $S(\omega,K_x,K_z)$ is uniform and includes the long wavelengths, the inverse problem is well-conditioned. Then, the model update will be close to 'true-amplitude' and FWI will easily converge to the true model. If, on the other hand, the sensitivity is highly non-uniform, the update will be related to a subset of the spatial frequencies. Although this may decrease the least-squares error substantially in the first few iterations, the model update will be quite different from the desired one and will slow down or even prevent convergence to the true model.

If the misfit functional is defined as the $L_2$ norm in the $(K_x,K_z)$ space, the squared sensitivity, $S^2(K_x,K_z)$, is proportional to the Hessian in the spatial wavenumber domain. The latter is diagonal if the background of the perturbation is locally homogeneous, assuming that we weight all the data uniformly in $(K_x,K_z)$ space. A different weighting can improve the sensitivities and therefore improve FWI convergence.

### Average sensitivities

To mimic time-domain inversion, we simply integrate the absolute value of the sensitivity normalized by source signature over the frequency range.

$$\mathbb{S}(K_x,K_z) = \int_{-\infty}^{\infty}|s(\omega)S(\omega,K_x,K_z)|\,d\omega \tag{9}$$

Single-frequency sensitivities as given by equation 8 are often oscillatory. We expect them to become more uniform if stacked over a number of frequencies, which is equivalent to simultaneous inversion of a number of frequencies. When the set of frequencies becomes dense, we effectively obtain the average sensitivity as encountered in time-domain inversion. The single-frequency sensitivities are simply scaled proportionally to frequency in the case of two halfspaces (Kazei et al., 2013b), as there is no scale parameter other than wavelength. With a free surface, layer thickness comes into play and the sensitivity in equation 8 depends on frequency in a more complicated way.




DOI http://dx.doi.org/10.1190/segam2015-5898847.1

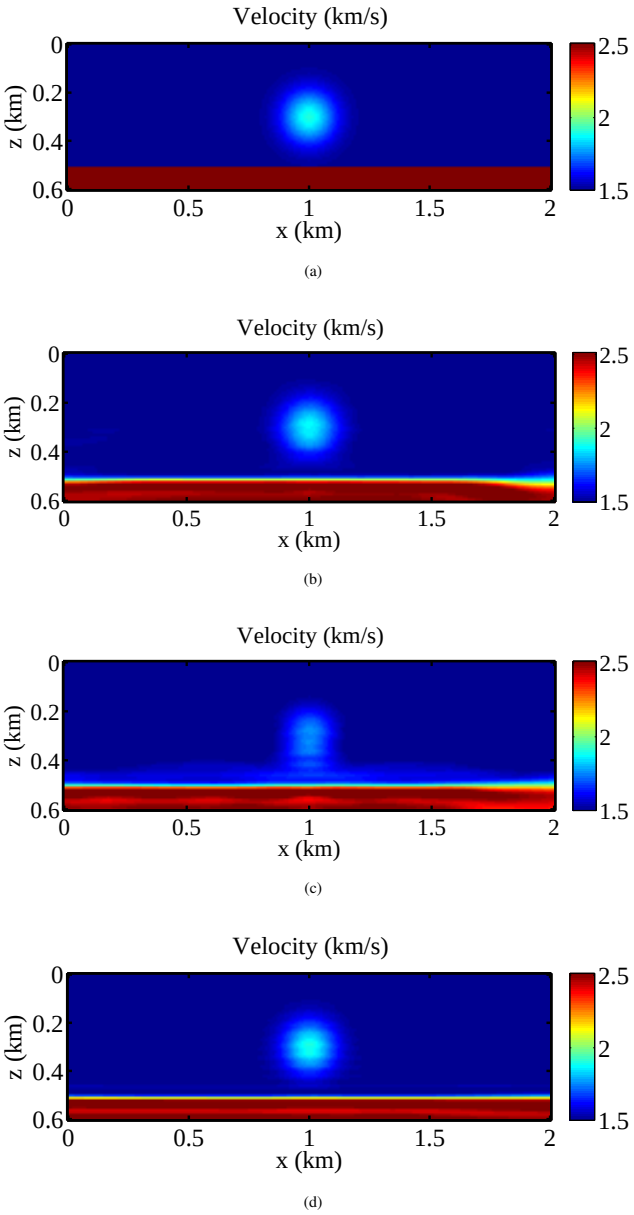


Figure 2: (a) True velocity model used to generate synthetic data for inversion. Modeling was performed without and with a free surface at zero depth. Sources and receivers were placed at a depth of 20 m. A Ricker wavelet with a peak frequency of 12 Hz was used as source wavelet. (b) Result after 94 L-BFGS iterations, using three frequencies of 3, 11 and 19 Hz, without a free surface. (c) Result with a free surface after 272 iterations, using the same frequencies. (d) Result after 179 iterations, using 81 equidistant frequencies between 3 and 19 Hz, which is almost the same as doing FWI in the time domain. We applied frequency-domain FWI, inverting with a single set of frequencies.

## SENSITIVITIES, FWI RESULTS & DISCUSSION

We performed a set of numerical experiments with a 2-D acoustic frequency-domain FWI code to figure out how many frequencies are needed to reconstruct a small Gaussian velocity perturbation in the model of two halfspaces 2(a). Starting from a model without the perturbation, 3 frequencies proved to be sufficient to reconstruct the velocity model of Figure 2(b) in the absence of a free surface, using rather long offsets up to 3 km for a perturbation at a depth of only 300 m. Next, we included the free surface that generates multiples and obtained the result of Figure 2(c). Figure 4 shows how the normal modes destroy the smooth character of the sensitivity spectra but improve the overall sensitivity when considering inversion for a velocity perturbation in the *upper* layer.

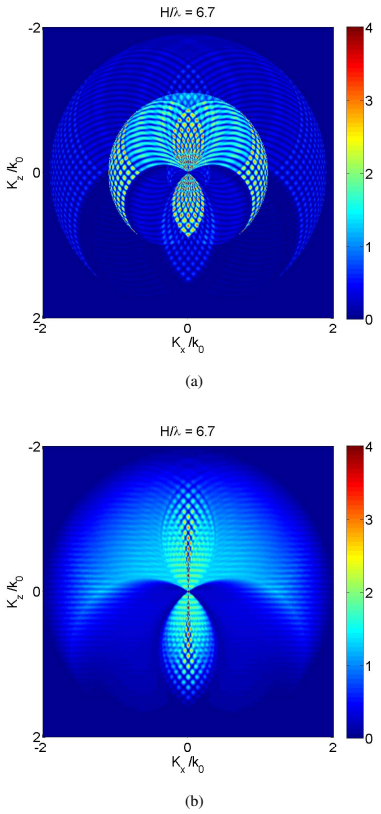


Figure 3: (a) Stacking of three frequencies patterns with frequency corrections is not sufficient to make the sensitivity more uniform. (b) Summation of the patterns over all frequencies effectively smooths the sensitivity. Normal modes of a fixed order have the same vertical components for different frequencies and these cause the horizontal stripes.

The criterion for existence of the first normal mode in case of a free layer over a halfspace is $H/\lambda \geq 1/(4\sqrt{1-(c_0/c_1)^2})$, where $H$ is the layer thickness and $\lambda = 2\pi c_0/\omega$ is the wavelength in the upper layer (Brekhovskikh and Godin, 1998). For $c_1/c_0 = 1.7$, the critical ratio $H/\lambda \simeq 0.3$, meaning that the first mode is just appearing in the right-upper panel of Figure 4, giving rise to peaks in several spots. Its interaction


DOI http://dx.doi.org/10.1190/segam2015-5898847.1

with the direct waves and total internal reflections produces additional bright circular arcs. Therefore, the first-order multiples bias the inversion towards a particular subset of spatial wavenumbers of the perturbation. Stacking over several frequencies is a natural way to regularize the problem, as shown in Figure 3(a). Since the positions of the maxima change with frequency, stacking appears to substantially improve the uniformity in coverage. The best option would be to emulate time-domain inversion, involving all frequencies at once. The sensitivities at low frequencies tend to be more uniform and are improved by the multiples for some small $K_z$ values (long vertical wavelengths). With increasing frequency, the panels are becoming highly oscillatory with many local maxima created by combinations of normal modes traveling at different angles.

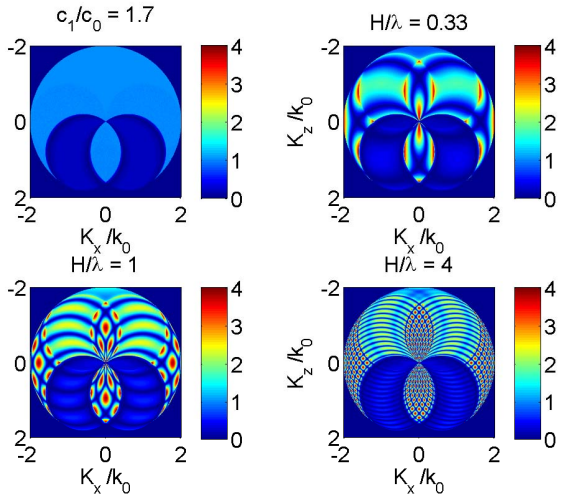


Figure 4: Sensitivities of the spatial wavefield spectrum to changes in the velocity spectrum in the upper layer at different frequencies. The left-upper panel shows the sensitivity pattern in the absence of a free surface. The other panels show sensitivities modified by the first-order multiples. These patterns are normalized by the maximum in the left-upper panel, corresponding to the case without multiples. If the layer thickness is taken as 500 m, then the right-upper panel corresponds to a very low frequency of 1.5 Hz and the left-lower panel to 3 Hz – the first frequency used for inversion. The right-lower panel corresponds to 12 Hz.

Normal modes do not penetrate into the deeper parts of the model, which strongly affects the sensitivities for those parts. They become more uniformly illuminated by leaking modes (Roth et al., 1998) only. The lower part of the figures can only be reached by upgoing waves that were reflected at least once from the deeper parts (Kazei et al., 2013b). If the perturbation is in the deeper halfspace and does not have any reflectors below, we lack illumination by upgoing waves and any hope to restore about one half of the perturbation spectrum is lost. Figure 5 illustrates the sensitivities in the wavenumber domain when the deepest reflector is present. Bright circles are provided by refracted waves traveling almost horizontally at the depth of the perturbation; this requires long offsets in the data.

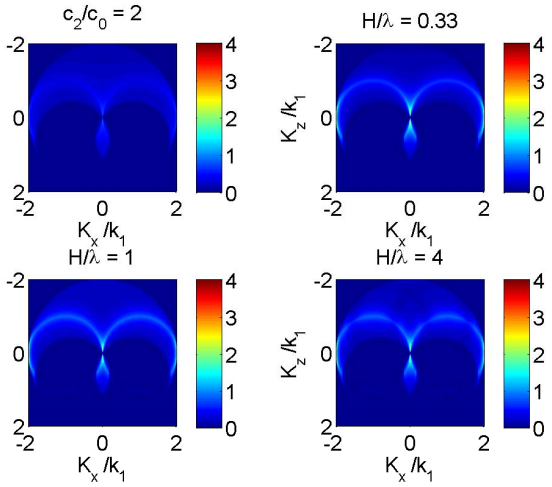


Figure 5: As Figure 4, but for a perturbation in the deeper halfspace, sketched in the Figure 1(b). We take only first-order reflections from the deepest reflector into account. This is sufficient to cover the whole spectrum in the idealized case when all offsets are present in the data.

These waves are boosted by leaking modes, making the circles more visible. Low vertical and horizontal wavenumbers are likely to be resolved better when multiples are included and the deeper part has a higher velocity than the upper.

## CONCLUSIONS

The spectral sensitivities technique shows that first-order multiples in the data contain useful information for full waveform inversion. If the free-surface multiples are generated by a reflector deeper than the target area for inversion, then normal modes affect the spectral relation, making single-frequency inversion more sensitive to a discrete subset of wavenumbers of the velocity model. This adversely affects convergence. Using multiple frequencies or time-domain FWI helps in the presence of multiples, because integration over frequencies effectively smooths the sensitivity patterns, given longer wavelengths a chance. If the area of interest is below the reflector that creates the multiples, the patterns are only affected by leaking modes which make refractions at close to horizontal angles stronger. Long-offset data are required to benefit from those waves in full-waveform inversion.

## ACKNOWLEDGMENTS

This project was proposed and supported by Fons ten Kroode of Shell Global Solutions International BV under CRDF grant RUG1-30020-ST-11. Additional support was provided by Saint Petersburg State University under research grant 11.38.217.2014. Research was carried out using computational resources provided by Resource Center "Computer Center of SPbU". The first author is grateful for helpful discussions to Jean Virieux, David Lumley and René-Edouard Plessix.




DOI http://dx.doi.org/10.1190/segam2015-5898847.1

**EDITED REFERENCES**

Note: This reference list is a copyedited version of the reference list submitted by the author. Reference lists for the 2015 SEG Technical Program Expanded Abstracts have been copyedited so that references provided with the online metadata for each paper will achieve a high degree of linking to cited sources that appear on the Web.

**REFERENCES**


Baeten, G., J. W. de Maag, R.-E. Plessix, R. Klaassen, T. Qureshi, M. Kleemeyer, F. ten Kroode, and Z. Rujie, 2013, The use of low frequencies in a full-waveform inversion and impedance inversion land seismic case study: Geophysical Prospecting, **61**, no. 4, 701–711. http://dx.doi.org/10.1111/1365-2478.12010.

Brekhovskikh, L. M., and O. A. Godin, 1998, Acoustics of layered media I: Plane and quasiplane waves: Springer.

Devaney, A. J., 1984, Geophysical diffraction tomography: IEEE Transactions on Geoscience and Remote Sensing, **GE-22**, no. 1, 3–13. http://dx.doi.org/10.1109/TGRS.1984.350573.

Kazei, V. V., B. M. Kashtan, V. N. Troyan, and W. A. Mulder, 2013a, Spectral sensitivity analysis of FWI in a constant-gradient background velocity model: 75th Annual International Conference and Exhibition, EAGE, Extended Abstracts, http://dx.doi.org/10.3997/2214-4609.20130599.

Kazei, V. V., V. N. Troyan, B. M. Kashtan, and W. A. Mulder, 2013b, On the role of reflections, refractions, and diving waves in full-waveform inversion: Geophysical Prospecting, **61**, no. 6, 1252–1263. http://dx.doi.org/10.1111/1365-2478.12064.

Mora, P., 1989, Inversion = migration tomography: Geophysics, **54**, 1575–1586. http://dx.doi.org/10.1190/1.1442625.

Roth, M., K. Holliger, and A. G. Green, 1998, Guided waves in near-surface seismic surveys: Geophysical Research Letters, **25**, no. 7, 1071–1074. http://dx.doi.org/10.1029/98GL00549.

Sirgue, L., and R. Pratt, 2004, Efficient waveform inversion and imaging: A strategy for selecting temporal frequencies: Geophysics, **69**, 231–248. http://dx.doi.org/10.1190/1.1649391.

Zhang, Y., G. Roberts, and A. Khalil, 2012, Compensating for source and receiver ghost effects in reverse-time migration: Presented at the 82nd Annual International Meeting, SEG.